Spin transfer torque in the presence of Andreev reflections

Shuai Wang and Ling Tang
State Key Laboratory for Surface Physics, Institute of Physics, Chinese Academy of Sciences, P.O. Box 603, Beijing 100190, China

Ke Xia
Department of Physics, Beijing Normal University, Beijing 100875, China

(Received 2 November 2009; revised manuscript received 3 February 2010; published 4 March 2010)

A first-principles method is developed to study the spin transfer torques in magnetic noncollinear textured ferromagnet-superconductor heterostructure. We apply the method to study the long-range spin-triplet pairing ($S_z = \pm 1$) induced by the spin-flip scattering near the ferromagnet-superconductor interface. The long-range spin-triplet Andreev reflection will saturate to the same value as usual Andreev reflection with strong enough spin-flip scattering. We find that the giant magnetoresistance effect of a spin valve with a superconductor contact can be restored by a small amount of interfacial spin-flip scattering.

DOI: 10.1103/PhysRevB.81.094404 PACS number(s): 72.25.−b, 74.45.+c, 71.15.Ap

I. INTRODUCTION

Ferromagnet-superconductor (F/S) heterostructures attract considerable interest recently.[1–6] The electron reflecting from F/S interfaces will gain a spin-dependent phase shift.[7] More interesting the long-range spin-triplet pairing ($S_z = \pm 1$) can be induced by the noncollinear magnetic texture[4,8,9] or magnetization precession.[5] Similar to the ferromagnet-normal-metal (F/N) heterostructure, the spin transfer torques[10,11] (STTs) also exist in the present of superconductor leads[12] but acquire new features in magnetic nanopillars connected to superconducting electrodes.[13] Experimentally, dc Josephson effect in SFNFS junctions has been reported.[1]

The basic concept of STTs is that spin angular momentum can be transferred by the flowing electrons from one ferromagnetic (FM) material to another FM, which is also identified experimentally by observation of the magnetization switching in FM spin valve.[14] The theories[15–18] combining the quantum treatment of the interface scattering and the Boltzmann-type treatment of the bulk scattering work reasonable well with the experiments of metallic system. Edwards *et al.*[19] and Haney *et al.*[20] performed full quantum mechanics calculation of STTs in spin valves by Green's-function-based formulism.

In fact, F/S interface has been a subtle topic in giant magnetoresistance (GMR) effect for many years.[21–23] Phase coherent theory predicted the absence of current perpendicular to the plane GMR due to Andreev reflection (AR) in F/S structure.[24] However, GMR has been observed in magnetic multilayers sandwiched between superconducting electrodes[25] and the measured interface resistance can be well compared with the numerical study[26] without considering AR. Spin-relaxation and spin-flip scattering could be the reason for the restoring the GMR effect in F/S system but whether GMR can be 100% restored is not clear.

AR measurements in normal-metal/superconductor (N/S) and F/S devices was carefully investigated[27] experimentally. The inelastic-scattering-induced pair-breaking effects were believed to be important in explaining the experiment observation. It is hard to compare experiment to the qualitative calculation directly due to the poorly formed F/S interfaces. The bcc Fe can be well matched with the fcc Al by rotating 45°. The interface between superconducting Al and ferromagnetic Fe is a good candidate for the detailed study of the AR spectrum of point contact.[2]

In this paper, we have generalized the first-principles scattering wave-function method[28] to include the AR within Bogoliubov-de Gennes[29] frame. With the scattering wave function, we calculate the conductance and STT. The rest of the paper is organized as following. In Sec. II, we present the details of the formalism for obtaining the scattering wave functions. In Sec. III, the formula of calculating the STT for electron and hole is presented. In Sec. IV, method is used to calculate the long-range spin-triplet AR due to the spin-flip scattering near Fe/Al interface. In Sec. V, we showed how the GMR in Fe/Ag/Fe/Al spin valves can be completely restored by a small amount of spin-flip scattering at the Fe/Al interface. In Sec. VI, we summarize our results.

II. FORMULA

Let us consider ferromagnetic nanopillars connected to a superconductor sketched in Fig. 1. The ferromagnetic moments are in general noncollinear. The Bogoliubov-de Gennes equation[29] can be written as

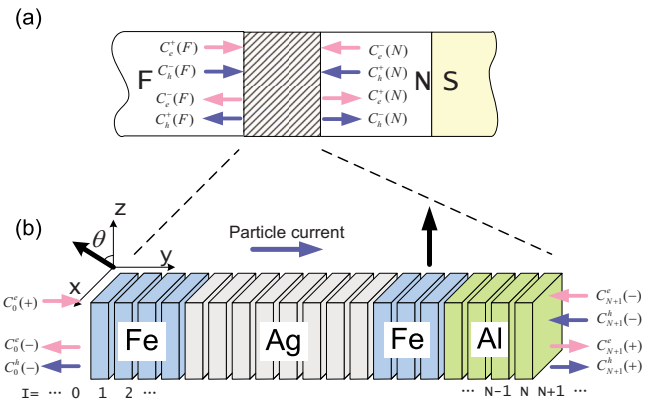

FIG. 1. (Color online) (a) The sketch of F/S junction with inserting a fictitious N metal region between F and S. (b) The sketch of Fe/Ag/Fe spin-valve structure connecting S contact with inserting a normal metal Al for technical convenience.

$$\begin{pmatrix} H_{0\uparrow\uparrow} & H_{0\uparrow\downarrow} & \Delta & 0 \\ H_{0\downarrow\uparrow} & H_{0\downarrow\downarrow} & 0 & \Delta \\ \Delta^* & 0 & -H^*_{0\downarrow\downarrow} & -H^*_{0\downarrow\uparrow} \\ 0 & \Delta^* & -H^*_{0\uparrow\downarrow} & -H^*_{0\uparrow\uparrow} \end{pmatrix} \begin{pmatrix} c_{e\uparrow} \\ c_{e\downarrow} \\ c_{h\downarrow} \\ c_{h\uparrow} \end{pmatrix} = \varepsilon \begin{pmatrix} c_{e\uparrow} \\ c_{e\downarrow} \\ c_{h\downarrow} \\ c_{h\uparrow} \end{pmatrix}, \quad (1)$$

where $H_{0\sigma\sigma'}(\sigma=\uparrow,\downarrow)$ is the single-electron Hamiltonian for noncollinear magnetic structure. The $c_{e\sigma}(c_{h\sigma})$ are the coefficient vectors of the wave function of electrons (holes) with spin index σ in some convenient bases. The Δ is the superconducting pair potential. The excitation energy ε is measured relative to the Fermi energy. Here we label the holes spin the same as corresponding empty electron states.

The electron Hamiltonian for noncollinear system in linear-muffin-tin-orbital (LMTO) basis[30,31] set $|RL\zeta\rangle$ in the α representation is a 2×2 matrix in spin space and can be written as

$$\mathbf{H}^{\alpha}_{\mathbf{R}L,\mathbf{R}'L'} = U_{\mathbf{R}}[\bar{C}^{\alpha}_{\mathbf{R}L}\delta_{\mathbf{R}'L'\mathbf{R}L} + \sqrt{\bar{\Delta}^{\alpha}_{\mathbf{R}L}} S^{\alpha}_{\mathbf{R}L,\mathbf{R}'L'} \sqrt{\bar{\Delta}^{\alpha}_{\mathbf{R}'L'}}] U^{\dagger}_{\mathbf{R}'}, \quad (2)$$

where $\mathbf{R}$ is the site index and L can be defined by $L\equiv(l,m)$. l and m are the azimuthal and magnetic quantum numbers, respectively. $\zeta=\uparrow(\downarrow)$ denotes that the basis is eigenstate in spin space, which is parallel (antiparallel) to spin-quantization axis. $\bar{C}^{\alpha}_{\mathbf{R}L}$ and $\bar{\Delta}^{\alpha}_{\mathbf{R}L}$ are 2×2 potential parameter matrices expanded in spin space and diagonal in the local coordinate system. Here the bars above potential parameters mean that in the local coordinate system.

The unitary rotation matrix at site $\mathbf{R}$ can be defined by

$$U_{\mathbf{R}}(\theta_{\mathbf{R}},\varphi_{\mathbf{R}}) = \begin{bmatrix} \cos\frac{\theta_{\mathbf{R}}}{2} e^{-i\varphi_{\mathbf{R}}/2} & -\sin\frac{\theta_{\mathbf{R}}}{2} e^{-i\varphi_{\mathbf{R}}/2} \\ \sin\frac{\theta_{\mathbf{R}}}{2} e^{i\varphi_{\mathbf{R}}/2} & \cos\frac{\theta_{\mathbf{R}}}{2} e^{i\varphi_{\mathbf{R}}/2} \end{bmatrix}, \quad (3)$$

where $\theta_{\mathbf{R}},\varphi_{\mathbf{R}}$ are the azimuth angles of the local quantization axis. Screened structure constants $S^{\alpha}_{\mathbf{R}L,\mathbf{R}'L'}$ contain all information about the structure, which are block diagonal in the spin space,

$$S^{\alpha}_{\mathbf{R}L,\mathbf{R}'L'} = s^{\alpha}_{\mathbf{R}L,\mathbf{R}'L'} \begin{bmatrix} 1 & 0 \\ 0 & 1 \end{bmatrix}. \quad (4)$$

$P^{\alpha}_{\mathbf{R}L}(\varepsilon)$ is the screened potential function matrix and contains all information about the atomic species at site $\mathbf{R}$ for calculating the electronic structure,

$$P^{\alpha}_{\mathbf{R}L}(\varepsilon) = U_{\mathbf{R}}\bar{P}^{\alpha}_{\mathbf{R}L}(\varepsilon)U^{\dagger}_{\mathbf{R}}. \quad (5)$$

The $\bar{P}^{\alpha}_{\mathbf{R}L}$ is diagonal in the local coordinate system,

$$\bar{P}^{\alpha}_{\mathbf{R}L}(\varepsilon) \equiv \begin{bmatrix} \bar{p}^{\alpha,\uparrow}_{\mathbf{R}L} & 0 \\ 0 & \bar{p}^{\alpha,\downarrow}_{\mathbf{R}L} \end{bmatrix}, \quad (6)$$

where $\bar{p}^{\alpha,\uparrow(\downarrow)}_{\mathbf{R}L} \equiv (E-\bar{C}^{\alpha,\uparrow(\downarrow)}_{\mathbf{R}L})(\bar{\Delta}^{\alpha,\uparrow(\downarrow)}_{\mathbf{R}L})^{-1}$.

Let us consider the system always has two-dimensional (2D) translational symmetry in the plane perpendicular to the transport direction. All the states can be characterized by a lateral wave vector $\mathbf{k}_{\parallel}$ in the corresponding 2D Brillouin zone (BZ). The screened Korringa-Kohn-Rostoker (KKR) equation[31] for electron in the mixed representation of $\mathbf{k}_{\parallel}$ and real-space layer index I [see Fig. 1(b)] is

$$-S^{\mathbf{k}_{\parallel}}_{I,I-1}\mathbf{C}^{e}_{I-1} + [P^{\alpha}_{I,I}(\varepsilon) - S^{\mathbf{k}_{\parallel}}_{I,I}]\mathbf{C}^{e}_{I} - S^{\mathbf{k}_{\parallel}}_{I,I+1}\mathbf{C}^{e}_{I+1} = 0. \quad (7)$$

Here, $\mathbf{C}_I \equiv C_{Ii} \equiv C_{IRlm\zeta}$ describes the wave-function amplitude in terms of some localized orbital basis where i labels the atomic orbital and atom site. $\mathbf{C}_I$ is a $2(l_{\max}+1)^2H \equiv 2M$ dimensional vector describing the amplitudes of the Ith layer with H sites and $2(l_{\max}+1)^2$ orbitals per site in the spin space. $P^{\alpha}_{I,I}$ and $S_{I,J}$ are $2M\times2M$ matrices. $P^{\alpha}_{I,I}=U_I\bar{P}^{\alpha}_{I}(\varepsilon)U^{\dagger}_{I}$ is matrix of potential functions characterizing the AS potentials of layer I similar to Eq. (5) and

$$S^{\mathbf{k}_{\parallel}}_{I,J} = \sum_{\mathbf{T}\in\{\mathbf{T}_{I,J}\}} S^{\alpha}(\mathbf{T}) e^{i\mathbf{k}_{\parallel}\cdot T}, \quad (8)$$

where $\{\mathbf{T}_{I,J}\}$ denotes the set of vectors that connect one lattice site in the Ith layer with all lattice sites in the Jth layer.

We also have to write down the equation of motion for the holes. To make use of the same KKR equation matrix as electrons, we write the KKR of the holes for its conjugate wave function as

$$-S^{\mathbf{k}_{\parallel}}_{I,I-1}\mathbf{C}^{h*}_{I-1} + [P^{\alpha}_{I,I}(-\varepsilon) - S^{\mathbf{k}_{\parallel}}_{I,I}]\mathbf{C}^{h*}_{I} - S^{\mathbf{k}_{\parallel}}_{I,I+1}\mathbf{C}^{h*}_{I+1} = 0. \quad (9)$$

The center problem of this paper is to solve scattering problem of the Bogoliubov-de Gennes equation in Eq. (1). Adapt the method by Beenakker,[32] we insert a fictitious N metal region between F and S, here the N metal is assumed to be the S in its normal state, see Fig. 1(a).

When $\Delta=0$, the Eq. (1) can be divided by two sets of equations for electrons and holes. The Bloch states of the normal-metal and ferromagnetic materials can be obtained and the wave functions of the electron and hole have the following symmetry:

$$\begin{pmatrix} c_{h\uparrow}(\varepsilon) \\ c_{h\downarrow}(\varepsilon) \end{pmatrix} = \begin{pmatrix} c^*_{e\uparrow}(-\varepsilon) \\ c^*_{e\downarrow}(-\varepsilon) \end{pmatrix}. \quad (10)$$

For a single F/N interface, the total incoming and outgoing scattering wave coefficients (electrons and holes) can be connected by the scattering matrix,

$$\begin{pmatrix} c^-_e(\mathrm{F}) \\ c^+_e(\mathrm{N}) \\ c^+_h(\mathrm{F}) \\ c^-_h(\mathrm{N}) \end{pmatrix} = \begin{pmatrix} r^e_{11} & t^e_{12} & 0 & 0 \\ t^e_{21} & r^e_{22} & 0 & 0 \\ 0 & 0 & r^h_{11} & t^h_{12} \\ 0 & 0 & t^h_{21} & r^h_{22} \end{pmatrix} \begin{pmatrix} c^+_e(\mathrm{F}) \\ c^-_e(\mathrm{N}) \\ c^-_h(\mathrm{F}) \\ c^+_h(\mathrm{N}) \end{pmatrix} \quad (11)$$

and this matrix can be obtained for realistic materials based on the local-density approximation.[26] At the N/S interface, we only consider the AR and then the coefficient $c^+_e(\mathrm{N})$, $c^+_h(\mathrm{N})$ and $c^-_e(\mathrm{N})$, $c^-_h(\mathrm{N})$ have the relations

$$c^-_e(\mathrm{N}) = \alpha c^-_h(\mathrm{N}) e^{i\phi}, \quad (12)$$

$$c^+_h(\mathrm{N}) = \alpha c^+_e(\mathrm{N}) e^{-i\phi}. \quad (13)$$

Here α describes the phase shift due to the penetration of the wave function into the superconductor. For $|\varepsilon|<\Delta_0$, $\alpha=\exp[-i\arccos(\varepsilon/\Delta_0)]$, $|\varepsilon|>\Delta_0$, $\alpha=[\varepsilon-\mathrm{sgn}(\varepsilon)\sqrt{\varepsilon^2-\Delta_0^2}]/\Delta_0$,

$\mathrm{sgn}(x)$ is the signal function. In this paper, we only consider the normal s-wave pair potential.

Considering an electron coming from left lead, denote the incoming wave function as $\mathbf{C}_0^e(+)$. Making use of the property of Bloch wave in the ideal leads, we can deduce the infinite coupled linear equation into finite serials of equations, the electron satisfies

$$\begin{pmatrix} \mathbf{C}_0^e \\ \mathbf{C}_1^e \\ \mathbf{C}_2^e \\ \cdots \\ \mathbf{C}_N^e \\ \mathbf{C}_{N+1}^e \end{pmatrix} = (\mathbf{P}-\tilde{\mathbf{S}})^{-1} \times \begin{pmatrix} \hat{S}_{0,-1}[F_L^{-1}(+)-F_L^{-1}(-)]\mathbf{C}_0^e(+) \\ 0 \\ 0 \\ \cdots \\ 0 \\ \hat{S}_{N+1,N+2}[F_R(-)-F_R(+)]\mathbf{C}_{N+1}^e(-) \end{pmatrix}. \quad (14)$$

The boundary condition on the right side changes comparing with the system of normal lead. We have, $\mathbf{C}_{N+1}^e(-) = \alpha^2(1-\alpha^2 r_{22}^* r_{22})^{-1} r_{22}^* t_{21} \mathbf{C}_0^e(+)$ and the hole's equation of motion can be written as

$$\begin{pmatrix} \mathbf{C}_0^{h*} \\ \mathbf{C}_1^{h*} \\ \mathbf{C}_2^{h*} \\ \cdots \\ \mathbf{C}_N^{h*} \\ \mathbf{C}_{N+1}^{h*} \end{pmatrix} = (\mathbf{P}-\tilde{\mathbf{S}})^{-1} \begin{pmatrix} 0 \\ 0 \\ 0 \\ \cdots \\ 0 \\ \hat{S}_{N+1,N+2}[F_R(-)-F_R(+)]\mathbf{C}_{N+1}^{h*}(-) \end{pmatrix} \quad (15)$$

with $\mathbf{C}_{N+1}^h(-) = \alpha e^{-i\phi}(1-\alpha^2 r_{22} r_{22}^*)^{-1} t_{21} \mathbf{C}_0^e(+)$.

The above linear equations can be solved by the Green's-function method developed early.[28] From the scattering wave function obtained, we get the incoming and reflecting waves relation as

$$\begin{pmatrix} c_e^-(\mathrm{F}) \\ c_h^+(\mathrm{F}) \end{pmatrix} = \begin{pmatrix} R_{ee} & R_{eh} \\ R_{he} & R_{hh} \end{pmatrix} \begin{pmatrix} c_e^+(\mathrm{F}) \\ c_h^-(\mathrm{F}) \end{pmatrix}. \quad (16)$$

Here the reflect matrix elements of the system are R_{ee} and R_{eh} can be obtained by wave function at zeroth layer ($\mathbf{C}_0^e$ and $\mathbf{C}_0^h$) and R_{he} and R_{hh} are defined with a hole comes from the left.

In the linear-response regime, the spectral conductance can be written as

$$G_{\mathrm{FS}}(\varepsilon) = \frac{e^2}{h}\mathrm{Tr}(1 - R_{ee}R_{ee}^\dagger + R_{he}R_{he}^\dagger) \quad (17)$$

which can be divided by three parts. It can be written as[33]

$$G_{\mathrm{FS}}(\varepsilon) = G_{\mathrm{QP}} + G_{\mathrm{AR}} + G_{\mathrm{NAR}}. \quad (18)$$

Here G_{QP}, G_{AR}, and G_{NAR} can be defined by

$$G_{\mathrm{QP}} \equiv \frac{e^2}{h}\mathrm{Tr}[1 - R_{ee}R_{ee}^\dagger],$$

$$G_{\mathrm{AR}} \equiv \frac{e^2}{h}\mathrm{Tr}[R_{he}^{\downarrow\uparrow}R_{he}^{\downarrow\uparrow\dagger} + R_{he}^{\uparrow\downarrow}R_{he}^{\uparrow\downarrow\dagger}],$$

$$G_{\mathrm{NAR}} \equiv \frac{e^2}{h}\mathrm{Tr}[R_{he}^{\downarrow\downarrow}R_{he}^{\downarrow\downarrow\dagger} + R_{he}^{\uparrow\uparrow}R_{he}^{\uparrow\uparrow\dagger}].$$

G_{QP} is the quasiparticle-contributed conductance. G_{AR} is the usual AR, which include the contribution from spin singlet and triplet ($S_z=0$) Andreev reflection.[34] G_{NAR} is the long-range spin-triplet component when the aligning magnetization vectors are noncollinear.

The AR spectrum can be calculated with scattering wave function and the well-established scattering matrix method.[32,35,36] These two calculations yield exactly the same results in our calculation. Instead of writing the STT in the language of Green's function,[20,37] we calculated the STT with the aid of the scattering wave functions of the scattering regime.[28,38]

III. TORQUES

With the scattering wave function we obtained, we can calculate spin current between $\mathbf{R}$th and $\mathbf{R}'$th sites ($\mathbf{R} \neq \mathbf{R}'$). The spin-current operator $\hat{\mathcal{J}}_{\mathbf{R}',\mathbf{R}}(\mathbf{k}_\parallel)$ from $\mathbf{R}'$th to $\mathbf{R}$th site ($\mathbf{R} \neq \mathbf{R}'$) can be written as[28]

$$\hat{\mathcal{J}}_{\mathbf{R}',\mathbf{R}}(\mathbf{k}_\parallel) = \sum_{LL'} \frac{1}{2i\hbar}[\hat{\sigma}\hat{\mathbf{H}}^{\mathbf{k}_\parallel}_{\mathbf{R}L,\mathbf{R}'L'} + \hat{\mathbf{H}}^{\mathbf{k}_\parallel}_{\mathbf{R}L,\mathbf{R}'L'}\hat{\sigma} - \mathrm{H.c.}], \quad (19)$$

where $\hat{\mathcal{J}}_{\mathbf{R}',\mathbf{R}}(\mathbf{k}_\parallel)$ is a vector in spin space.

For a specific state $|\Psi^{\mathbf{k}_\parallel}\rangle$, define $\langle\hat{\mathbf{O}}\rangle \equiv \langle\Psi^{\mathbf{k}_\parallel}|\hat{\mathbf{O}}|\Psi^{\mathbf{k}_\parallel}\rangle$, $\langle\hat{\mathbf{T}}^s_{\mathbf{R}}(\mathbf{k}_\parallel)\rangle$ can be defined as the difference of the incoming spin current and outgoing spin current of $\mathbf{R}$ site in the Ith principal layer,

$$\langle\hat{\mathbf{T}}^s_{\mathbf{R}}(\mathbf{k}_\parallel)\rangle = \sum_{\mathbf{R}'\in I-1,I} \langle\hat{\mathcal{J}}^s_{\mathbf{R}',\mathbf{R}}(\mathbf{k}_\parallel)\rangle - \sum_{\mathbf{R}'\in I,I+1} \langle\hat{\mathcal{J}}^s_{\mathbf{R},\mathbf{R}'}(\mathbf{k}_\parallel)\rangle, \quad (20)$$

where the superscript s is used to denote that the incoming state is parallel or antiparallel to the local spin-quantization axis of injection lead. After summation over 2D BZ, STTs acted on $\mathbf{R}$th atom can be expressed as

$$\mathbf{T}_{\mathbf{R}} = \left(\frac{\hbar}{2}\right)\frac{e}{h}\frac{1}{N_\parallel}\sum_{s,\mathbf{k}_\parallel}\langle\hat{\mathbf{T}}^s_{\mathbf{R}}(\mathbf{k}_\parallel)\rangle V_b, \quad (21)$$

where the bias is given by the difference between the electrochemical potentials of the two leads as $eV_b = \mu_L - \mu_R$.

In the presence of AR, the total STTs come from electron and holes contributions,

$$\mathbf{T_R} = \mathbf{T}^e_{\mathbf{R}}(+) + \mathbf{T}^h_{\mathbf{R}}(-).$$

Here +(−) denotes direction of incoming wave function from left (right) lead. $\mathbf{T}^e_{\mathbf{R}}(+)$ is calculated with the wave function obtained by Eq. (14). $\mathbf{T}^h_{\mathbf{R}}(-)$ corresponds to the wave function obtained with Eq. (15). Due to the electron and hole symmetry, we have $\mathbf{T}^h_{\mathbf{R}}(-) = -\mathbf{T}^e_{\mathbf{R}}(-)$.

The out-of-plane STT in the normal state can be obtained by taking the STT of right-going electrons minus STT of the left-going holes in linear-response limit.[28,39–41] In the presence of AR, how to describe the left-going holes from superconductor region became complicated. We do not attempt to discuss the out-of-plane torque component in this paper.

IV. ANDREEV REFLECTION ($S_z = \pm 1$) DUE TO THE INTERFACIAL SPIN-FLIP SCATTERING

Let us start from Fe/Al (001) interface. The bulk Al has fcc crystal structure with lattice constants 4.05 Å. The bulk Fe has bcc crystal structure with lattice constants 2.87 Å. The fcc Al lattice and bcc Fe lattice can be well matched in the (001) direction, by rotating fcc Al lattice 45° around (001) axis. The mismatch of this structure is less than 1%. In the paper, we chose the lattice constants of bulk Al unchanged and the Fe lattice been compressed slightly to match the Al. The distance of ideal Fe/Al (001) interface can be determined as following. The interfacial cubic unit cell consists 0.5 Fe atom and 0.5 Al atom, where these Fe and Al atoms should fill up the space of the cubic with volume $V = d \times (a_{\mathrm{Fe}}/2)^2$. The other distance of between Al-Al and Fe-Fe monolayers (MLs) remain the same as the bulk values.

Using the tight-binding (TB)-LMTO SGF method[30] and the ASA (Ref. 31) technique, we start by calculating self-consistent potentials of an interface embedded between two semi-infinite Fe and Al leads. Here we use the density-functional theory in local spin-density approximation[30] and take the exchange-correlation potential of von Barth-Hedin parameterization.[42] The electron is treated scalar relativistic and the cutoff of orbital angular momentum of basis is $l_{\max} = 2$, corresponding to *spd* basis. The transport calculations are carried out with a $\mathbf{k}_{\parallel}$-mesh density equivalent to 4900 $\mathbf{k}_{\parallel}$-mesh points in the 2D BZ of a 1×1 interface unit cell.

For disorder Fe/Al (001) interface, we use the coherent-potential approximation[30] to calculate the charge and spin densities at the disordered alloy interface $Fe_{0.5}Al_{0.5}$. We also assume the distance of two interfacial Fe and Al ML is same as the case of ideal interface. The disorder interface of Fe/Al (001) is modeled by 2 ML 50–50 % alloyed with Al atoms and Fe atoms at interfacial layers. The other parameters are the same with the case of ideal interface. After obtaining the effective potential for the Fe and Al at disorder interface, in AR calculation an $H = H_1 \times H_2$ lateral supercell[43] is constructed in which the potentials are randomly distributed, maintaining the concentration for which they were self-consistently calculated.

The conductance of Fe/Al (001) interfaces in the present of magnetic misalignment is shown in Fig. 2. Here we define $g(V) \equiv [G_{\mathrm{FS}}(V) - G_{\mathrm{FN}}(0)]/G_{\mathrm{FN}}(0)$, where $G_{\mathrm{FN}}(0)$ is the normal-state conductance and $G_{\mathrm{FS}}(V)$ is the differential conductance for an F/S interface at finite bias. The magnetic misalignments are introduced by Gaussian random distributions of magnetic moments orientations near the interface. The deviation angle between local quantum axis and global quantum axis within the 7×7 lateral supercell satisfies the Gaussian random distribution with the average orientation is along global quantum axis and the distribution width is $\Delta\theta$. For ideal interface in Fig. 2(a), there are two subgap peaks at $E/\Delta = \pm 0.94$ and the minimum of conductance is at zero bias. Here ideal means there is no any interfacial alloy in the calculation. These subgap resonances are very sensitive to the spin-dependent phase shift at the F/S interface and the detail were discussed by Cottet and Belzig.[7]

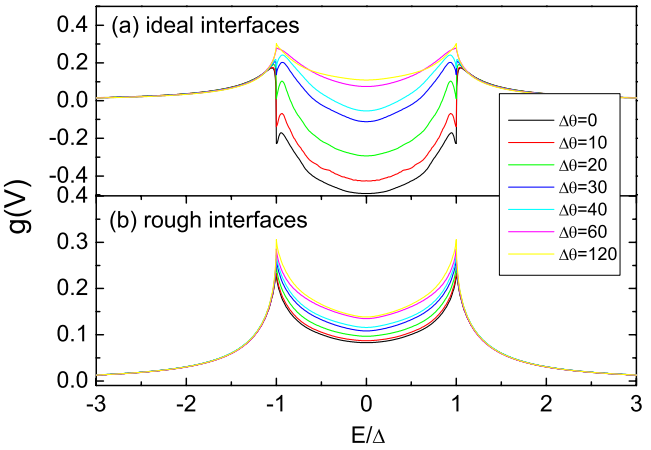

FIG. 2. (Color online) The normalized conductance spectral for different spin-flip scattering ratio ($\Delta\theta$) through Fe/Al (001) with (a) ideal interface and (b) rough interface.

When we take the interfacial alloy into account in Fig. 2(b), the subgap resonance were washed out by random spin-dependent phase-shift gain at the Fe/Al interface. The maximum of conductance curve is at the edge of energy gap ($\varepsilon/\Delta_0 = \pm 1$) and the conductance at zero bias is the minimum value.

The conductance due to usual and long-range spin-triplet AR of disordered Fe/Al (001) at zero bias is shown in Fig. 3(a). The G_{AR} is zero without spin-flip scattering ($\Delta\theta = 0$). With increasing the magnetization misalignment, $G_{\mathrm{NAR}}(S_z = \pm 1)$ increases rapidly while the G_{AR} decreases. This is due to the spin-flip scattering at the interface. For the distribution width $\Delta\theta > 60°$ the long-range spin-triplet AR has been saturated which is corresponding to the saturation of spin-flip probability at interface.

When the distribution width $\Delta\theta > 60°$, the conductance due to G_{NAR} is close to the G_{AR} and is about the half of the G_{AR} in $\Delta\theta = 0$ case.

The relation between long-range spin-triplet pairing ($S_z = \pm 1$) and the spin-flip process at interface can be understood as following. Defined spin-flip ratio through a F/N interface as $P \equiv (G^{\uparrow\downarrow}_{\mathrm{F/N}} + G^{\downarrow\uparrow}_{\mathrm{F/N}})/(G^{\uparrow\uparrow}_{\mathrm{F/N}} + G^{\downarrow\downarrow}_{\mathrm{F/N}})$. Here $G^{\uparrow\uparrow}$ and $G^{\downarrow\downarrow}$ are conductance through F/N for majority and minority electron channel without spin-flip scattering and $G^{\uparrow\downarrow}(G^{\downarrow\uparrow})$ is conductance of spin-flip process. Let us consider electrons with majority spin coming from left side and passing through F/N interface. The ratio of transmitted majority-spin electron is

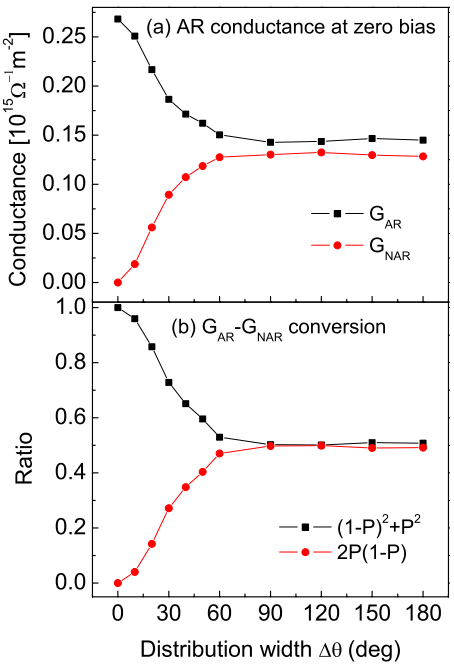

FIG. 3. (Color online) (a) The G_{AR} and G_{NAR} Andreev conductance through Fe/Al (001) as a function of $\Delta\theta$ with rough interface at zero bias. (b) The G_{AR} and G_{NAR} conversion according to the spin-flip ratio P as a function of distribution width $\Delta\theta$.

$(1-P)$ and that of minority spin is P. Assuming no spin-flip process at N/S interface, the ratio of AR hole with majority spin is P and that of minority spin is $(1-P)$. These left going holes will pass through the F/N interface again and with the same spin-flip ratio. As a result, in the ferromagnetic region the ratio of reflection hole with majority spin is $P(1-P)+(1-P)P$ and the ratio of minority-spin hole is $P^2+(1-P)^2$. Therefore the G_{AR} is proportional to $P^2+(1-P)^2$ and $G_{NAR}(S_z=\pm 1)$ is proportional to $2P(1-P)$. Figure 3(b) shows $P^2+(1-P)^2$ and $2P(1-P)$ as function of $\Delta\theta$. From Figs. 3(a) and 3(b) it can be seen that the above argument can well describe the conversion between G_{AR} and G_{NAR}.

V. Fe/Ag/Fe/Al (001) SPIN VALVE

In this section, we will show how the GMR effect can be restored by the interface spin-flip scattering. The modeling system we used is Fe/Ag/Fe/Al (001) spin valve with the polarization direction θ, see Fig. 1(b). Bulk Ag is fcc crystal structure with lattice constants 4.09 Å, which are very close to that of Al. In the calculation, we chose the lattice constants of bulk Al(4.05 Å) as lattice constants parallel to the layers. The distance between Fe and Ag at the Fe/Ag interface is chosen the same as that of Fe/Al interface. The disordered interface is modeled by 2 ML 50–50 % interfacial alloy. The other parameters are chosen the same as that of Fe/Al (001) interface.

Figure 4 shows how the GMR can be restored by the interface spin-flip scattering in realistic materials. Here the GMR is defined as $\mathrm{GMR} \equiv [G(0°)-G(180°)]/G(0°)$. Top three panels are the zero-bias conductance through Fe/Ag/Fe/Al (001) as the function of the relative angle θ with N and S contacts.

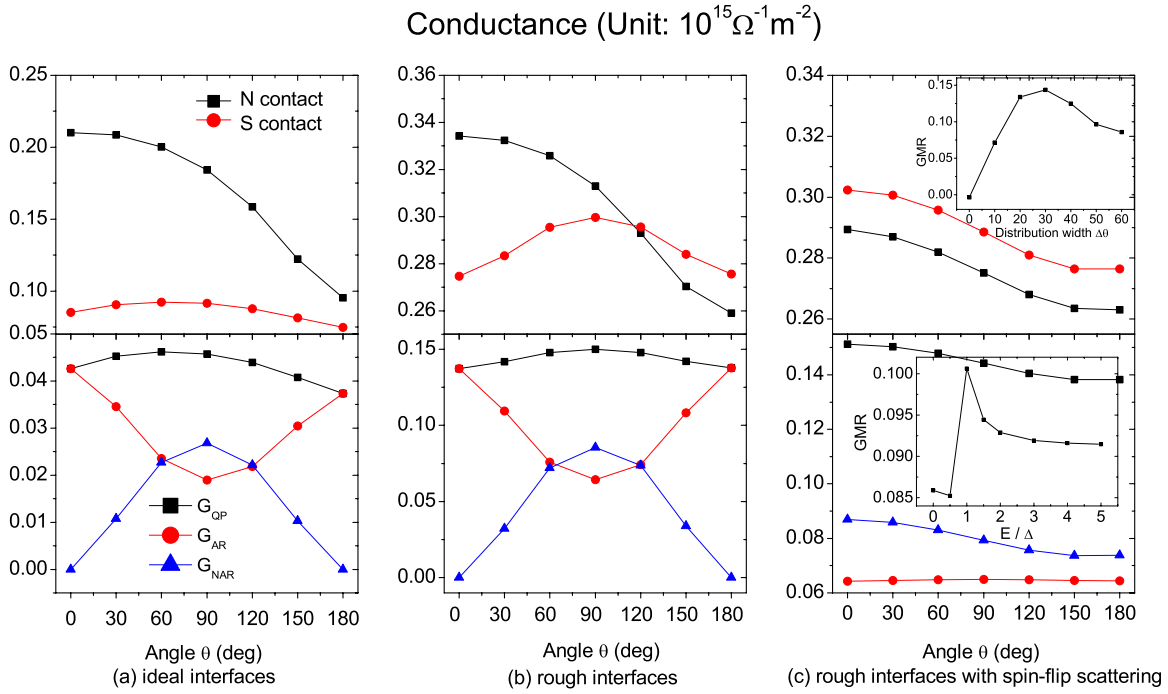

FIG. 4. (Color online) Top three panels are the zero-bias conductance through Fe/Ag/Fe/Al (001) as the function of relative angle θ with N and S contacts. Three panels are (a) ideal interfaces, (b) rough interfaces, and (c) rough interfaces with spin-flip scattering $\Delta\theta=60°$. The separate contribution from Andreev conductance is shown in the bottomed panel. They are G_{QP}, G_{AR}, and G_{NAR}. The inset of the top panel in (c) shows GMR of Fe/Ag/Fe/Al (001) at zero bias as a function of distribution width $\Delta\theta$. The inset of the bottom panel in (c) represents the GMR of Fe/Ag/Fe/Al (001) as a function of energy with $\Delta\theta=60°$ and relative angle $\theta=60°$.

For the ideal interface, as shown in Fig. 4(a), there is only very small conductance difference between parallel and antiparallel states in the presence of AR. As discussed by Taddei *et al.*,[24] the AR makes each ferromagnetic layer is passed twice, one by majority-spin electron (hole) and another by minority-spin hole (electron). The small GMR survived is due to the interference effect between interfaces. The separate contributions are shown in the bottomed panels. GMR between parallel and antiparallel states comes from G_{QP} and G_{AR}. As expected, contribution from the G_{NAR} is zero. Because there is no long-range spin-triplet pairing ($S_z=\pm 1$) AR when the magnetizations are all aligned collinearly.

When the interfaces are rough, as shown in Fig. 4(b), the random-phase shifts due to the interface scattering washed out all this interference effect, which result in zero GMR between parallel and antiparallel states. The $G_{NAR}(S_z=\pm 1)$ is maximum for $\theta=90°$ while the G_{AR} is minimum as expected. The total conductance yields small angular dependence.

Figure 4(c) shows the conductances as the function of relative angle θ between magnetization when the interface is rough and with spin-flip scattering. The interface spin-flip scattering is modeled by a Gaussian distribution of the magnetic moments near the Fe/Al interface. The magnetic orientation distribution width is $\Delta\theta=60°$ and the averaged direction is point to the direction of the magnetization of other layers. The $\Delta\theta=60°$ is close to the theory calculation of noncollinear magnetic structure in ferromagnet/metal interface.[44] There is not much difference between two curves, which means that the GMR effect at zero bias is complete restored in the present of the AR with enough spin-flip scattering. As the relative angle θ between magnetization changing from 0° to 180°, the contribution from G_{AR} does not change much and the contribution from $G_{NAR}(S_z=\pm 1)$ changes about 14%.

The inset of the top panel in Fig. 4(c) shows the zero-bias GMR effect of Fe/Ag/Fe/Al (001) with different distribution width $\Delta\theta$. Surprisingly, GMR can be restored with small amount spin-flip scattering and GMR does not change monotonically with $\Delta\theta$. The GMR reaches maximum value when $\Delta\theta=30°$ in our calculation.

The inset of the bottom panel in Fig. 4(c) shows the GMR effect of Fe/Ag/Fe/Al (001) with distribution width $\Delta\theta=60°$ and relative angle $\theta=60°$ as a function of energy. The GMR has the similar shape to the normalized conductance, see Fig. 2(b).

Next we will see how the STTs changed by the AR. Let us focused on the zero bias at first, Fig. 5(a) shows in-plane STT of the free layers as a function of relative θ with N and S contacts. Here free layer is the Fe layer embedding between Ag and Al and all the interfaces contain 2 ML 50–50 % interfacial alloy. The free-layer STTs as the function relative angle θ is very similar to the Co/Cu/Co/Cu results[28] when Al is in normal state. However, the symmetry of the in-plane STT changes in the present of AR. It tends to be symmetric between θ and $180-\theta$, which has been predicted by modeling study.[45] The AR does not change the magnitude of the STTs much compare without AR.

The spin-flip scattering can restore the normal STT feature even in the present of AR. Figure 5(b) shows the in-plane STT on free layer as a function of θ with and without AR. Here the in-plane STT summed over all the layers with considering noncollinear magnetic moments. With considering the spin-flip scattering, there is almost no difference between two curves. When $\theta=0$ or 180, the in-plane STT is not zero because of the existing noncollinear aligned magnetic moments.

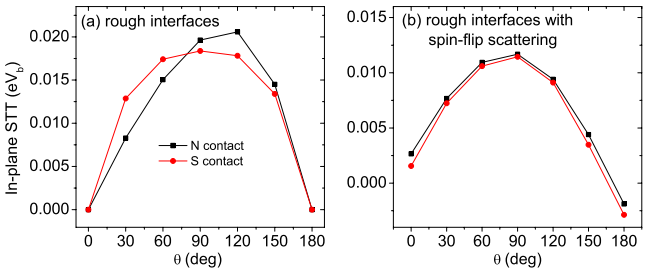

FIG. 5. (Color online) The in-plane STT as a function of relative θ for Fe/Ag/Fe/Al with (a) rough interface and (b) rough interface with spin-flip scattering $\Delta\theta=60°$. Here the contact can be N and S state.

The spectrum of the in-plane STT can also be obtained. Figure 6 gives in-plane STT as a function of the energy in the present of AR. Here relative angle is chosen as $\theta=60°$. Figure 6(a) shows the in-plane STT with rough interface but without spin-flip scattering. Figure 6(b) gives the in-plane STT of the same structure but with spin-flip scattering. STT spectrums could have the quite different feature compare with that of conductance spectrum in Fig. 2.

VI. SUMMARY

In summary, we have developed a method to study the STTs in magnetic noncollinear textured F/S heterostructure with realistic electron structure. The method is used to study the spin-flip scattering-induced long-range spin-triplet AR and GMR effect in the present of AR. The long-range spin-triplet pairing ($S_z=\pm 1$) induced by the spin-flip process at Fe/Al (001) interface can be understood quantitatively in our calculation. For spin-valve structure Fe/Ag/Fe/Al (001) with S contact, the GMR effect can be restored by a small amount of interface noncollinear alignments.

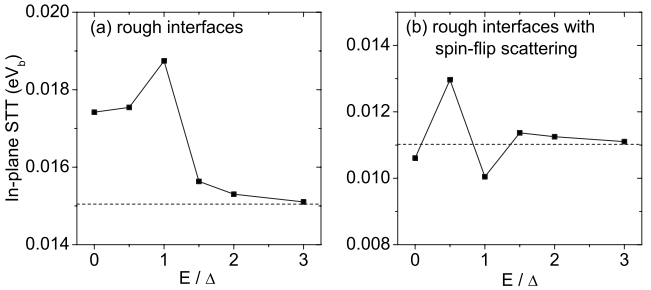

FIG. 6. The in-plane STT as a function of energy for Fe/Ag/Fe/Al with (a) rough interface and (b) rough interface with spin-flip scattering $\Delta\theta=60°$. Here the relative angle is chosen as $\theta=60°$. The dot lines denote the in-plane STT with N contacts.

ACKNOWLEDGMENTS

This work is supported by NSF of China (Grants No. 60825405 and No. 10774175) and MOST of China (Grant No. 2006CB933000). We are grateful to: Yong Wang for useful discussion; Ilja Turek for his TB-LMTO-SGF layer code which we used to generate self-consistent potentials; Anton Starikov for permission to use his version of the TB-MTO code based upon sparse matrix techniques with which we can solve Eqs. (14) and (15) in an efficient way.

[1] C. Bell, S. Milikisyants, M. Huber, and J. Aarts, Phys. Rev. Lett. **100**, 047002 (2008).
[2] M. Stokmaier, G. Goll, D. Weissenberger, C. Sürgers, and H. v. Löhneysen, Phys. Rev. Lett. **101**, 147005 (2008).
[3] V. Braude and Ya. M. Blanter, Phys. Rev. Lett. **100**, 207001 (2008).
[4] F. Konschelle and A. Buzdin, Phys. Rev. Lett. **102**, 017001 (2009).
[5] T. Yokoyama and Y. Tserkovnyak, Phys. Rev. B **80**, 104416 (2009).
[6] E. Zhao and J. A. Sauls, Phys. Rev. B **78**, 174511 (2008).
[7] A. Cottet and W. Belzig, Phys. Rev. B **72**, 180503 (2005); **77**, 064517 (2008).
[8] F. S. Bergeret, A. F. Volkov, and K. B. Efetov, Phys. Rev. Lett. **86**, 4096 (2001).
[9] J. Linder and A. Sudbø, Phys. Rev. B **75**, 134509 (2007).
[10] J. Slonczewski, J. Magn. Magn. Mater. **159**, L1 (1996).
[11] L. Berger, Phys. Rev. B **54**, 9353 (1996).
[12] J. Linder, T. Yokoyama, and A. Sudbo, Phys. Rev. B **79**, 224504 (2009).
[13] X. Waintal and P. W. Brouwer, Phys. Rev. B **65**, 054407(R) (2002).
[14] M. Tsoi, A. G. M. Jansen, J. Bass, W.-C. Chiang, M. Seck, V. Tsoi, and P. Wyder, Phys. Rev. Lett. **80**, 4281 (1998); M. Tsoi, A. G. M. Jansen, J. Bass, W.-C. Chiang, V. Tsoi, and P. Wyder, Nature (London) **406**, 46 (2000); E. B. Myers, D. C. Ralph, J. A. Katine, R. N. Louie, and R. A. Buhrman, Science **285**, 867 (1999).
[15] X. Waintal, E. B. Myers, P. W. Brouwer, and D. C. Ralph, Phys. Rev. B **62**, 12317 (2000).
[16] A. Brataas, Y. V. Nazarov, and G. E. W. Bauer, Phys. Rev. Lett. **84**, 2481 (2000); Eur. Phys. J. B **22**, 99 (2001).
[17] M. D. Stiles and A. Zangwill, J. Appl. Phys. **91**, 6812 (2002).
[18] M. D. Stiles and A. Zangwill, Phys. Rev. B **66**, 014407 (2002).
[19] D. M. Edwards, F. Federici, J. Mathon, and A. Umerski, Phys. Rev. B **71**, 054407 (2005).
[20] P. M. Haney, D. Waldron, R. A. Duine, A. S. Núñez, H. Guo, and A. H. MacDonald, Phys. Rev. B **76**, 024404 (2007).
[21] M. J. M. de Jong and C. W. J. Beenakker, Phys. Rev. Lett. **74**, 1657 (1995).
[22] S. K. Upadhyay, A. Palanisami, R. N. Louie, and R. A. Buhrman, Phys. Rev. Lett. **81**, 3247 (1998).
[23] R. J. Soulen, Jr., J. M. Byers, M. S. Osofsky, B. Nadgorny, T. Ambrose, S. F. Cheng, P. R. Broussard, C. T. Tanaka, J. Nowak, J. S. Moodera, A. Barry, and J. M. D. Coey, Science **282**, 85 (1998).
[24] F. Taddei, S. Sanvito, J. H. Jefferson, and C. J. Lambert, Phys. Rev. Lett. **82**, 4938 (1999).
[25] W. P. Pratt, Jr., S.-F. Lee, J. M. Slaughter, R. Loloee, P. A. Schroeder, and J. Bass, Phys. Rev. Lett. **66**, 3060 (1991).
[26] K. Xia, P. J. Kelly, G. E. W. Bauer, I. Turek, J. Kudrnovský, and V. Drchal, Phys. Rev. B **63**, 064407 (2001).
[27] P. Chalsani, S. K. Upadhyay, O. Ozatay, and R. A. Buhrman, Phys. Rev. B **75**, 094417 (2007).
[28] S. Wang, Y. Xu, and K. Xia, Phys. Rev. B **77**, 184430 (2008).
[29] P. G. de Gennes, *Superconductivity of Metals and Alloys* (Addison-Wesley, Reading, MA, 1966).
[30] I. Turek, V. Drchal, J. Kudrnovský, M. Šob, and P. Weinberger, *Electronic Structure of Disordered Alloys, Surfaces and Interfaces* (Kluwer, Boston, London, Dordrecht, 1997).
[31] O. K. Andersen, O. Jepsen, and D. Glötzel, in *Highlights in Condensed Matter Theory*, edited by F. Bassani, F. Fumi, and M. P. Tosi (North-Holland, Amsterdam, 1985), p. 59.
[32] C. W. J. Beenakker, Rev. Mod. Phys. **69**, 731 (1997).
[33] Z. P. Niu and D. Y. Xing, Phys. Rev. Lett. **98**, 057005 (2007).
[34] F. S. Bergeret, A. F. Volkov, and K. B. Efetov, Rev. Mod. Phys. **77**, 1321 (2005).
[35] G. B. Lesovik, A. L. Fauchère, and G. Blatter, Phys. Rev. B **55**, 3146 (1997).
[36] K. Xia, P. J. Kelly, G. E. W. Bauer, and I. Turek, Phys. Rev. Lett. **89**, 166603 (2002).
[37] Christian Heiliger, Michael Czerner, Bogdan Yu. Yavorsky, Ingrid Mertig, and Mark D. Stiles, J. Appl. Phys. **103**, 07A709 (2008).
[38] P. A. Khomyakov, G. Brocks, V. Karpan, M. Zwierzycki, and P. J. Kelly, Phys. Rev. B **72**, 035450 (2005).
[39] C. Heiliger and M. D. Stiles, Phys. Rev. Lett. **100**, 186805 (2008).
[40] D. C. Ralph and M. D. Stiles, J. Magn. Magn. Mater. **320**, 1190 (2008).
[41] I. Theodonis, N. Kioussis, A. Kalitsov, M. Chshiev, and W. H. Butler, Phys. Rev. Lett. **97**, 237205 (2006).
[42] U. von Barth and L. Hedin, J. Phys. C **5**, 1629 (1972).
[43] K. Xia, M. Zwierzycki, M. Talanana, P. J. Kelly, and G. E. W. Bauer, Phys. Rev. B **73**, 064420 (2006).
[44] A. B. Oparin, D. M. C. Nicholson, X. -G. Zhang, W. H. Butler, W. A. Shelton, G. M. Stocks, and Y. Wang, J. Appl. Phys. **85**, 4548 (1999).
[45] X. Waintal and P. W. Brouwer, Phys. Rev. B **63**, 220407(R) (2001).